

Electronic structure of a buried NiSi₂ or CoSi₂ layer in bulk Si

J. T. Schick

Department of Physics, Villanova University, Villanova, Pennsylvania 19085

S. M. Bose

Department of Physics and Atmospheric Science, Drexel University, Philadelphia, Pennsylvania 19104

(Received 9 November 1995; revised manuscript received 6 February 1996)

An empirical tight-binding Green's function model is applied to a single layer of nickel disilicide or cobalt disilicide embedded in bulk silicon. The electronic band structure of localized and extended states in the vicinity of the bulk silicon band gap is investigated. [S0163-1829(96)09119-9]

I. INTRODUCTION

Recently there has been much discussion on transition metal disilicides, especially NiSi₂ and CoSi₂, which are of particular interest because of the potential for use in Si devices.¹ These materials exhibit the fluorite structure with bulk lattice parameters close to those of Si, which allows the formation of nearly abrupt interfaces between these disilicides and Si.² Samples of Si/CoSi₂/Si heterostructures and films of CoSi₂ on silicon have been fabricated and studied in some detail³⁻⁹ with disilicide layer thicknesses down to about 2.6 nm, which corresponds to approximately seven layers of the disilicide. In a more applied vein, thin films of CoSi₂ embedded in silicon for use as Ohmic contacts in optoelectronic devices such as multijunction photovoltaic energy converters have recently been investigated.¹⁰

Because of this trend to approach microscopically thin films on surfaces or buried in bulk materials, we have chosen to model the limiting situation of a single plane of metal disilicide embedded in a perfect sample of silicon oriented in the (111) direction. We investigate the localized electronic states that result from this structure which will alter the bulk band gap in the vicinity of the embedded plane and will have profound effects on conduction in that neighborhood.

Empirical tight-binding calculations are performed because of the relative speed of results that has allowed us to take advantage of desktop computers which are readily available. Additionally, this approach allows us to easily avoid potential problems with periodicity which may be an issue in small supercell calculations. In the rest of this paper we briefly discuss our method, including the improvements we have made, in Sec. II and the results of band structure calculations in Sec. III.

II. COMPUTATIONAL MODEL

The model for computing Si band structures is the tight-binding approximation as used previously by Engle, Sulston, and Bose¹¹ (ESB) in their work on the electronic structure of the arsenic-passivated silicon (111) surface. In the ESB work the bulk Si model is similar to that of Chadi and Cohen¹² with the addition of two second-nearest-neighbor interaction terms to improve the lower conduction bands of the bulk material. Parameters for the buried layer of NiSi₂ are taken

from the calculation by Sulston and Bose,¹³ in which silicon interfaces with NiSi₂ and CoSi₂ were studied. Sulston and Bose found that the band structures and density of states for these disilicides were well represented within the tight-binding approximation, which is primarily due to the covalent nature of the bonding in these particular disilicides.¹⁴ Parameters from these calculations are summarized in Tables I and II.

In this calculation we have extended the Green's function theory of Kalkstein and Soven¹⁵ to the problem of a single buried layer of disilicide in bulk silicon. This method has been used previously by us in studying electronic structures at surfaces and interfaces of CdTe and HgTe.¹⁶ The central point of the model is that the effect of a surface, interface, buried layer, or other defect in a material can be included, if the bulk Green's function and the scattering potential due to the perturbation are known, through the use of a Dyson equation,

$$G' = G + GVG', \quad (1)$$

where G and G' are the bulk and defect system Green's functions, respectively. The scattering potential $V = H' - H$ is determined from the Hamiltonian for the bulk system H

TABLE I. Tight-binding parameters for bulk Si as used here and in Ref. 11.

Parameter	Value (eV)
$E_{s,s}(000)$	-5.79
$E_{s,s}(110)$	0.0945
$E_{x,x}(000)$	1.24
$E_{x,x}(011)$	-0.375
$E_{x,x}(110)$	0.181
$E_{s,s}\left(\frac{1}{2} \frac{1}{2} \frac{1}{2}\right)$	-2.0575
$E_{s,x}\left(\frac{1}{2} \frac{1}{2} \frac{1}{2}\right)$	1.00
$E_{x,x}\left(\frac{1}{2} \frac{1}{2} \frac{1}{2}\right)$	0.42875
$E_{x,y}\left(\frac{1}{2} \frac{1}{2} \frac{1}{2}\right)$	1.35

TABLE II. Tight-binding parameters for bulk metal disilicides from Ref. 13. The symbol M stands for the metal atom.

Parameter	NiSi ₂ value (eV)	CoSi ₂ value (eV)
$E_{s,s}(000)_M$	1.035	3.291
$E_{xy,xy}(000)_M$	-4.925	-3.761
$E_{z2,z2}(000)_M$	-4.94	-3.96
$E_{s,s}(000)_{Si}$	-7.4425	-7.1695
$E_{x,x}(000)_{Si}$	-0.1375	-0.1915
$E_{s,s}\left(\frac{1}{2}\frac{1}{2}\frac{1}{2}\right)_{M,Si}$	-0.9655	-0.978
$E_{s,x}\left(\frac{1}{2}\frac{1}{2}\frac{1}{2}\right)_{M,Si}$	0.210 75	0.126 75
$E_{xy,s}\left(\frac{1}{2}\frac{1}{2}\frac{1}{2}\right)_{M,Si}$	-0.6095	-0.712 75
$E_{xy,x}\left(\frac{1}{2}\frac{1}{2}\frac{1}{2}\right)_{M,Si}$	0.1875	0.382 25
$E_{xy,z}\left(\frac{1}{2}\frac{1}{2}\frac{1}{2}\right)_{M,Si}$	0.5305	0.641 25
$E_{xy,x}\left(\frac{1}{2}\frac{1}{2}\frac{1}{2}\right)_{M,Si}$	-0.254 75	-0.354 75
$E_{z2,x}\left(\frac{1}{2}\frac{1}{2}\frac{1}{2}\right)_{M,Si}$	0.110 25	0.1535
$E_{z2,z}\left(\frac{1}{2}\frac{1}{2}\frac{1}{2}\right)_{M,Si}$	-0.3	-0.45
$E_{s,s}(200)_{Si}$	-0.973 75	-1.075 25
$E_{s,x}(200)_{Si}$	1.485	1.655
$E_{x,x}(200)_{Si}$	2.911 25	2.885 75
$E_{x,x}(002)_{Si}$	-1.163 75	-1.228 25

and for the defect system H' . In computing G' , we must evaluate the inverse of the matrix $D = [1 - GV]$. Zeros of the determinant of the matrix D determine positions of localized states of the system, aiding interpretation of our results.

As a result of the periodic nature of the system in directions parallel to the surface and the broken symmetry perpendicular to the surface, we describe the system in terms of parallel wave vector \mathbf{k}_{\parallel} and layer number n . The Green's functions here are expressed in this mixed representation and the local density of states ρ_n is computed from the Green's function G through the use of

$$\rho_n(E, \mathbf{k}_{\parallel}) = -\frac{1}{\pi} \text{Im}[G(E, n, n, \mathbf{k}_{\parallel})]. \quad (2)$$

For the details of the methodology used in this paper the reader is referred to Refs. 11, 13, and 16. In this work we took the interactions between atoms within the buried layer to be unchanged from the values used for bulk NiSi₂ or CoSi₂. Interactions between silicon atoms in the disilicide layer and silicon atoms in the neighboring pure crystal were taken to be the same as in bulk silicon. Previously ESB (Ref. 11) observed that only small changes in the band structure result when off-diagonal second-neighbor interactions for the

silicon s and p orbitals are included, so we have chosen not to include these second-neighbor interactions in this calculation. The layer of metal disilicide is embedded in the bulk silicon so that the silicon in the buried layer forms single bonds to the silicon lattice. The metal atoms bond directly with silicon atoms of the buried layer as a result of the nearest-neighbor interactions used in this calculation. This arrangement corresponds to the sevenfold type-A interface structure, which is the generally accepted arrangement for nickel disilicide.^{17,18}

Green's functions for the bulk material are computed at energy values spaced 0.01 eV apart with an imaginary part to the energy of 0.05 eV. After the buried layer Green's functions have been found by the method prescribed above we analytically continue the result back to zero imaginary energy, through the use of a technique due to Hass, Velicky, and Ehrenreich,¹⁹ in order to search for localized states. The primary advantage to using this procedure is in the reduction in time needed to numerically evaluate the integrals for the matrix elements of the Green's functions while preserving all features in the local densities of states (LDOS).

III. RESULTS

First we discuss the LDOS in the vicinity of the buried layer in which there is no relaxation of the atoms or planes

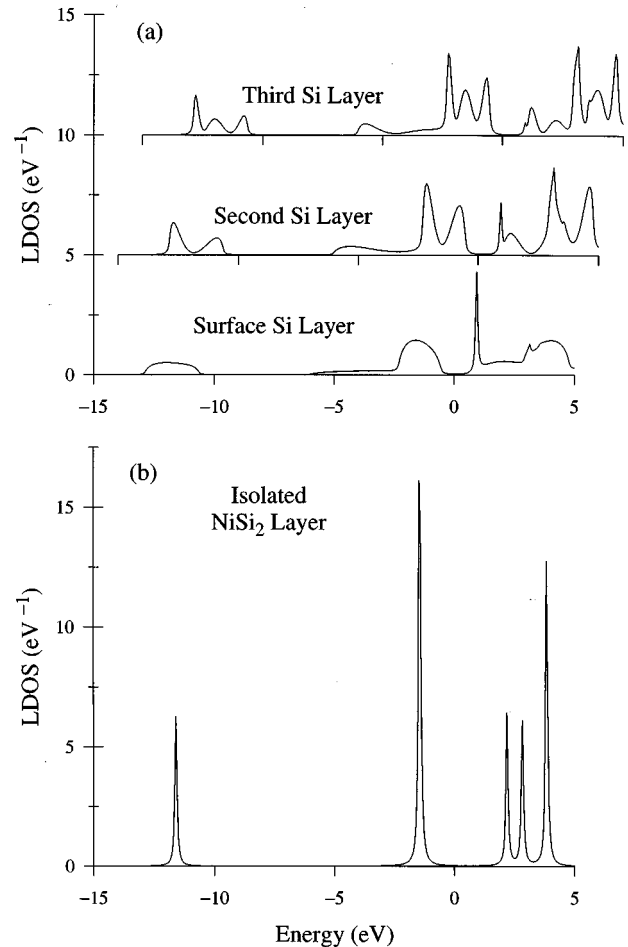


FIG. 1. LDOS for localized and extended states in (a) the first three layers of a truncated bulk Si surface and (b) an isolated layer of NiSi₂. A finite imaginary component of 0.05 eV is used in these plots.

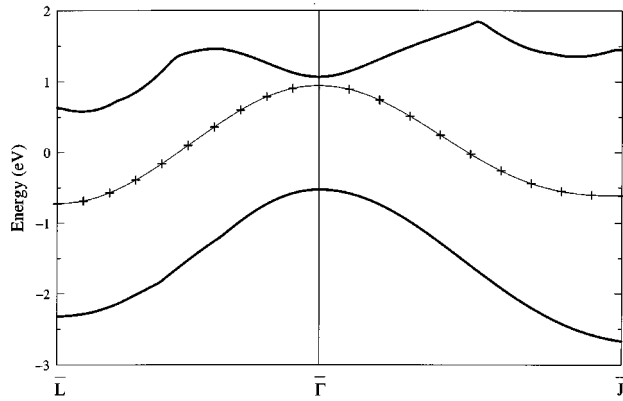


FIG. 2. Band structure of localized states for truncated (111) Si surface plotted against the bulk band edges. Zero energy is at the middle of the gap. Calculations were performed for the positions marked +; the smooth curves are drawn as a guide for the eye.

allowed. For comparison we present the LDOS calculated at $\bar{\Gamma}$ for the Si crystal truncated at the position of the buried layer. It should be pointed out that the LDOS plots in this section have not been smoothed as in earlier calculations (Ref. 11), but that the source of oscillations in those calculations, the use of interpolation of the band structure from values saved in computer memory, has been eliminated in our new code. Here we compute the energy levels as they are needed in the calculation. This has resulted not only in greatly improved LDOS but also in much reduced consumption of computer time, allowing us to perform our calculations on desktop computers.

The truncated silicon surface state can be seen as a peak high in the gap in Fig. 1. The width of the peaks is due to the finite imaginary component of energy used here, 0.05 eV. We note that the heights of surface states, which indicate

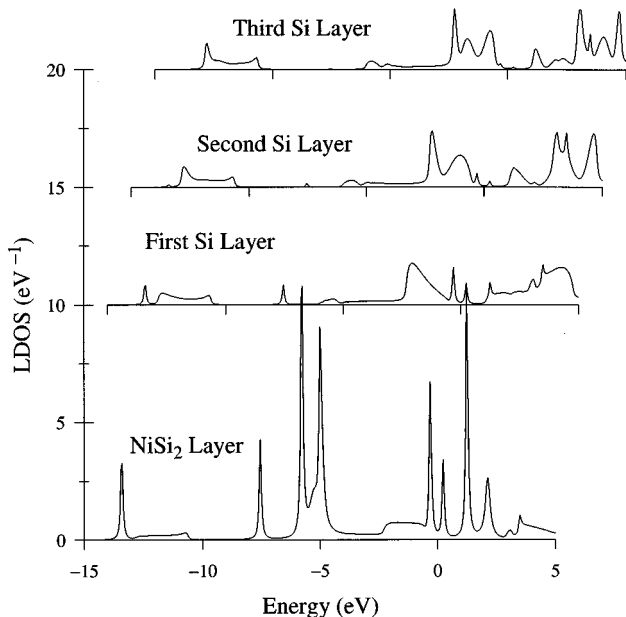


FIG. 3. Local densities of states for a NiSi_2 buried layer and the next three layers of Si. This interface is oriented in the (111) direction and an imaginary component of energy of 0.05 eV is used for these plots.

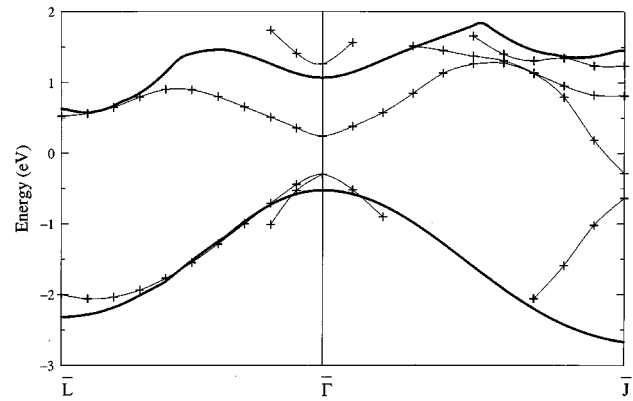


FIG. 4. Band structure of localized states in the gap of Si for the NiSi_2 buried layer in Si. Calculations performed at points indicated by +.

strength, decrease as we proceed to layers deeper in the crystal, as they must by definition. Additionally, we see that the LDOS takes on bulk characteristics by layer three and we have verified that by layer ten the LDOS shows most of the same features observed in the bulk. In Fig. 1(b) we show the LDOS of a single isolated layer of NiSi_2 . As a result of the lack of interactions with neighboring planes, we find that all the states associated with the disilicide layer are single peaks for a given value of \mathbf{k}_{\parallel} , indicating they are all localized on the plane as expected. Again, the heights are indicative of strength of the states.

In Fig. 2 we plot the band structure of the localized state for the silicon surface against the background of projected bulk band edges. The state, which appears high in the gap at the $\bar{\Gamma}$ point, is just a few tenths of an eV above the valence band maximum at \bar{L} and \bar{J} . This is in good qualitative agreement with the pseudopotential calculations of Elices *et al.*²⁰ as well as with tight-binding calculations of Pandey and Phillips.²¹

Turning our attention to a buried layer of nickel disilicide in silicon shown in Fig. 3, we find a significantly modified LDOS from that of the silicon surface/isolated disilicide layer seen in Fig. 1. The buried NiSi_2 layer develops bands and gaps in the LDOS corresponding to those in the adjacent silicon layers. However, at this layer the band gap is substantially altered because of two extra peaks, one in the vicinity of the center of the bulk silicon band gap and one low in the gap. Additionally, there is apparently a state resonant with the conduction band minimum; however, a closer examination of the matrix D , discussed above, reveals that this is not a true localized state. The localized nature of the remaining states is clear from the behavior of D and corroborated by the dependence of their strength on layer; i.e., the further from the buried layer we are, the lower the peak. Again, it can be seen that by the third layer the LDOS take on a largely bulk character. In the vicinity of the NiSi_2 layer the optical properties of these samples will obviously be very different from those of pure Si and such altered properties are very important for technological applications.

In Fig. 4 we present the band structure of localized states for the buried layer against the background of projected bulk band edges. Note that these states are quite different in number and position from those obtained from the Si surface

calculations, which is not surprising in light of the different sources of the states. All bands are found to consist of a mixture of s and p states of Si or s and d states of the metal. The midgap state at $\bar{\Gamma}$ primarily consists of the s and p states of Si and d states of Ni. The pair of bands low in the gap near $\bar{\Gamma}$, which are seen to merge with the bulk band structure, are strongly comprised of Si p states with the lower band exhibiting some Si and Ni s character. The degeneracy in the bands is accidental and would be removed by a slightly different choice of interaction potentials. The high energy band in the neighborhood of $\bar{\Gamma}$ and resonant with the conduction band shows contributions of the Si p states with significant amounts of the Ni d and s states present. In the region between $\bar{\Gamma}$ and \bar{J} where there are two bands in proximity to and above the midgap band, there is a very strong Ni s character with some Si s character on the band just above the midgap band. The highest band also has a great deal of Ni s character but involves a more significant contribution of Si p states. The lowest band near \bar{J} is nearly the same in character to the state that merges into the band near $\bar{\Gamma}$. Note that up to four states are evident in the band gap around \bar{J} .

The situation is nearly the same in the case of CoSi_2 (see Fig. 5), but we see that the bands are generally higher in the gap, especially in the case of the "midgap" band which now appears about 0.5 eV below the conduction band edge at $\bar{\Gamma}$. Additionally, the pair of bands present near $\bar{\Gamma}$ at low energy are similar in character to those for NiSi_2 . The state highest in the gap near \bar{J} has strong contributions from Si s and p states and Co d states with the addition of some Co s character.

IV. CONCLUSION

In this paper we have examined the effect on the electronic structure of a bulk Si sample when a single layer of

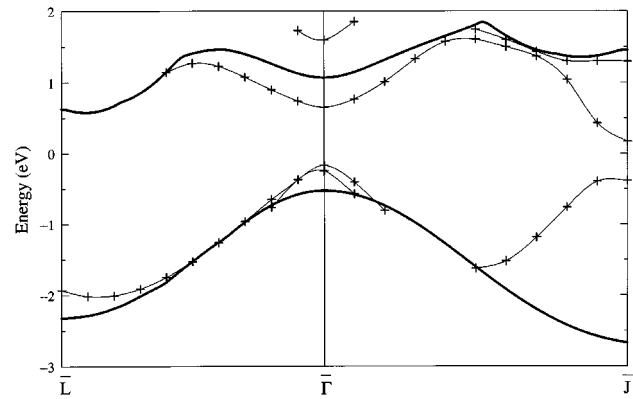


FIG. 5. Band structure of localized states in the gap of Si for the CoSi_2 buried layer in Si. Calculations performed at points indicated by +.

nickel or cobalt disilicide is embedded in the (111) orientation. Using the tight-binding Green's function method to study the energy region from the upper valence band of silicon through the lower conduction band we see that states localized on the defect plane appear in the gap primarily near the band edges. Such localized states will have an effect on conduction in the vicinity of the disilicide if the bulk material is doped n type, which would lead to the potential trapping of charge carriers in the silicon near the buried layer.

ACKNOWLEDGMENTS

This work was supported by NASA/JPL Grant No. 958144.

¹S. P. Murarka, *J. Vac. Sci. Technol.* **17**, 775 (1980).

²R. T. Tung, *Phys. Rev. Lett.* **50**, 429 (1983).

³F. Lu, C. H. Perry, and F. Namavar, *J. Appl. Phys.* **75**, 7465 (1994).

⁴J. Y. Duboz, P. A. Badoz, E. Rosencher, J. Hertz, M. Ospelt, H. von Känel, and A. Briggs, *Appl. Phys. Lett.* **53**, 788 (1988).

⁵J. R. Jimenez, Z.-C. Wu, L. J. Schowalter, B. D. Junt, R. W. Fathauer, P. J. Grunthaler, and T. L. Lin, *J. Appl. Phys.* **66**, 2738 (1989).

⁶J. Y. Duboz, P. A. Badoz, J. Henz, and H. von Känel, *J. Appl. Phys.* **68**, 2346 (1990).

⁷M. Wölfel, M. Schulz, J. Ionally, and P. J. Grunthaler, *Appl. Phys. A* **50**, 177 (1990).

⁸Z.-C. Wu, E. T. Arakawa, J. R. Jimenez, and L. J. Schowalter, *J. Appl. Phys.* **71**, 5601 (1992).

⁹M. Müller, D. Bahr, and W. Press, *J. Appl. Phys.* **74**, 1590 (1993).

¹⁰N. M. Kalkhoran, H. P. Maruska, and R. Namavar, *Appl. Phys.*

Lett. **64**, 1980 (1994).

¹¹W. P. Engle, K. W. Sulston, and S. M. Bose, *Phys. Rev. B* **50**, 10 880 (1994).

¹²D. J. Chadi and M. L. Cohen, *Phys. Status Solidi B* **68**, 405 (1975).

¹³K. W. Sulston and S. M. Bose, *J. Phys. Condens. Matter.* **3**, 7607 (1991).

¹⁴J. Tersoff and D. R. Hamann, *Phys. Rev. B* **28**, 1128 (1983).

¹⁵D. Kalkstein and P. Soven, *Surf. Sci.* **26**, 85 (1971).

¹⁶J. T. Schick, S. M. Bose, and A.-B. Chen, *Phys. Rev. B* **40**, 7825 (1989).

¹⁷D. R. Hamann, *Phys. Rev. Lett.* **60**, 313 (1988).

¹⁸G. Li and S. Rabii, *Phys. Rev. B* **49**, 2927 (1994).

¹⁹K. C. Hass, B. Velicky, H. Ehrenreich, *Phys. Rev. B* **29**, 3697 (1984).

²⁰M. Elices, F. Flores, E. Louis, and J. Rubio, *J. Phys. C* **7**, 3020 (1974).

²¹K. C. Pandey and J. C. Phillips, *Phys. Rev. Lett.* **32**, 1433 (1974).